

## CHAPTER 3

### MODELING ROTAVATOR TORQUE AND POWER REQUIREMENTS

#### 3.1 Introduction

The changing location of the tip of a rotavator as it processes the soil is one of the key parameters that must be considered when developing a mathematical model for its torque requirements. For a rotavator fitted with cutting blades of given a configuration, the instantaneous location of its tip is determined by the kinematics of the rotavator. This change in depth, as the blade processes the soil, results in continuous change of the torque requirements from the initiation to the end of the soil cutting process. Rotavator kinematics affects the choice of the renovator's design and operational parameters, which in turn have a marked effect on its torque requirements.

With the exception of the direction of rotation, which affects the shape of the cut soil slice, all the other rotavator input parameters (Figure 1.2) can be held constant for a given setup. For the two possible directions of rotation on a horizontal rotor (Figure 1.1a), two mathematical models can be developed for predicting the variation of torque requirements with the angle of rotation or instantaneous depths for a chosen cutting blade configuration. This arises because the soil-tool interactions for the down- and up-cutting directions of rotation are different.

In this study, only the down-cut direction was considered for modelling the rotavator torque requirements. The down-cut direction of rotation was preferred because of the following reasons:

- reverse rotational rotavators are uncommon
- the forward thrust generated by a down-cut rotavator aids in traction
- the instantaneous behaviour of the blade is similar to that of an inclined passive blade, therefore the existing force prediction models can be modified in the development of their torque and specific energy prediction models.

The first part of this chapter analyzes the kinematics of a down-cutting rotavator. The remainder of the chapter is devoted to the development of an analytical model for predicting the force, torque and energy requirements for a down-cutting rotavator fitted with L-shaped blades.

### 3.2 Rotavator kinematics

Rotavators execute combined rotational and forward motion during tillage operations. The path of motion of each point on the rotavator tine depends on the circumferential and forward travel velocities, as well as the direction of rotation. An understanding of the rotavator kinematics is necessary for the analysis of its operations (Hendrick & Gill, 1971a). Kinematics is the study of motion without, reference to the force(s) causing the motion (Meriam & Kraige, 1987).

#### 3.2.1 Equation of motion and the cutting trajectory of the tiller blade

In rotavators, the forced rotation of the rotor shaft, with working tools fixed to it, participates in two motions, namely, the rotary motion around its axis with velocity  $V_{cir}$  and forward travel speed,  $V_f$ , associated with the prime-mover e.g. a tractor. For deriving the equation of motion, a stationary system of co-ordinates (Figure 3.1) is considered.

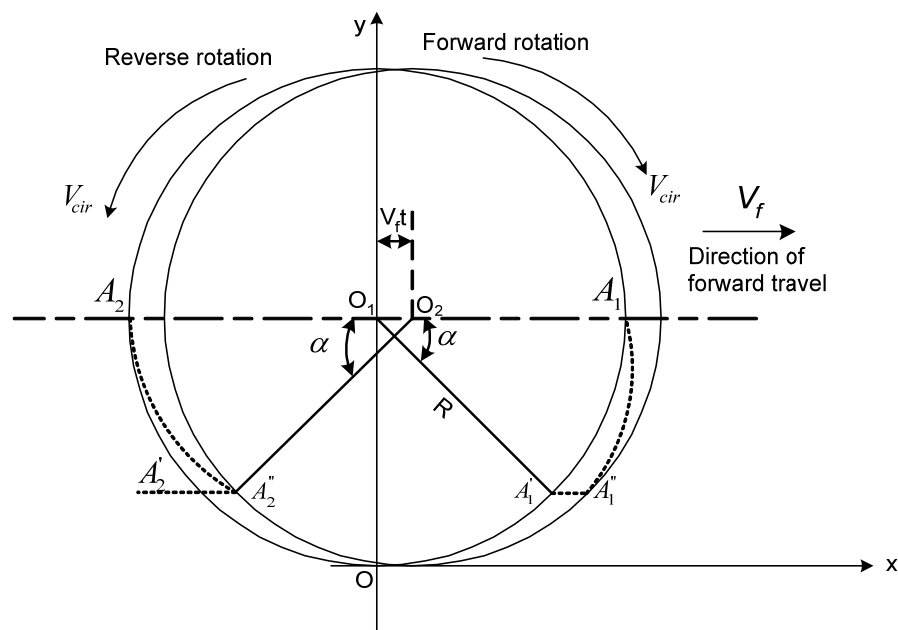


**Figure 3.1:** Diagram for the determination of the equation of motion (Sineokov & Panov, 1978).

Let the rotor of radius,  $R$ , turn through an angle,  $\alpha$ , from its original position in time,  $t$  (Figure 3.1). The point  $A_1$ , for the case of down-cut rotation; and point  $A_2$ , for the case of the up-cut rotation, corresponding with the tip of the tiller blade, take positions  $A_1'$  and  $A_2'$ , respectively, for a stationary system. In practice, the system is not stationary and a point on the rotor tiller travels along a path that is a combination of the forward travel speed and the rotor rotational speed. In this case, the distance from the rotational axis to the point of interest points,  $A_1'$  and  $A_2'$ , move a distance equal to  $V_f \cdot t$ , and take positions  $A_1''$  and  $A_2''$ , respectively. The co-ordinates of these points are expressed (Hendrick & Gill, 1971a; Bernacki *et al.*, 1972 and Sineokov & Panov, 1978) as:

$$\left. \begin{aligned} x &= V_f t \pm R \cos \alpha \\ y &= R(1 - \sin \alpha) \end{aligned} \right\} \dots (3.1)$$

where:

$\alpha$  = the angle of rotation of the tiller blade with respect to its initial position (rad.)

$t$  = is the time of rotation of the rotor through angle  $\alpha$  (s).

Equation (3.1) determines the absolute trajectory of motion of rotavator blades with a horizontal axis of rotation. Geometrically, this trajectory is a trochoid or curate cycloid (Figure 3.2) depending on the distance of the point from the rotor axis (Hendrick & Gill, 1978; Bernacki *et al.*, 1972; Bosoi *et al.*, 1988; and Sineokov & Panov, 1978).

While Equation (3.1) could be used for design purposes, the parameter most frequently used, both as a design and use parameter, is the dimensionless ratio of the rotor peripheral velocity ( $V_{cir}$ ) to the machine forward travel velocity ( $V_f$ ) called the kinematic parameter,  $\lambda$ , (Hendrick & Gill, 1971c). This dimensionless ratio is expressed as:

$$\lambda = \frac{V_{cir}}{V_f} = \frac{R\omega}{V_f} \dots (3.2)$$

where:

$R$  = rotor radius (m)

$\omega$  = angular velocity of the rotor (rad/s)

$V_f$  = forward travel velocity (m/s).

$V_{cir}$  = peripheral velocity of the rotor blades (m/s)

Substituting the value of  $\lambda$  into Equation (3.1) gives the trajectory of motion of the tiller blades as:

$$\left. \begin{aligned} x &= R \left( \frac{\alpha}{\lambda} \pm \cos \alpha \right) \\ y &= R (1 - \sin \alpha) \end{aligned} \right\} \dots (3.3)$$

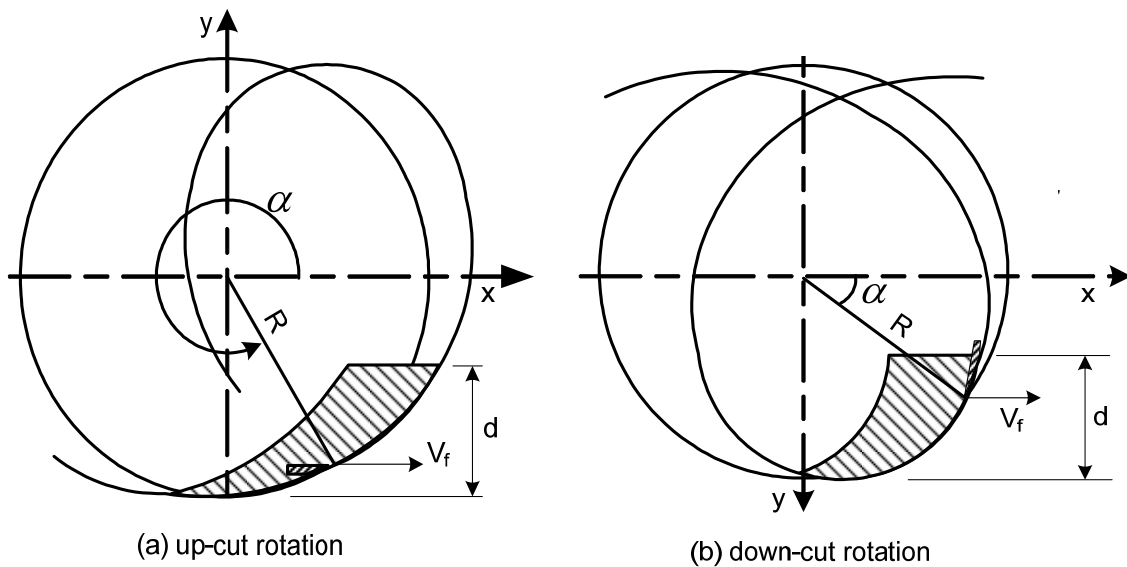


**Figure 3.2:** Trajectories of working elements and thickness of shapes of the soil slices cut by rotavator blades during up- and down-cut tillage (Hendrick & Gill, 1971a)

Equation (3.3) shows that the variation of the trochoidal shape is affected only by  $\lambda$ , characterising the working regime of rotavators. Figure 3.3 presents the dimensions and form of the cut slices of soil as determined by trajectories of two successively working tines and their direction of rotation. From Figure 3.3, the direction of rotation of the blades, relative to the travel direction, also influences the rotavator working regime.

The tilling speed or the absolute velocity of the tiller blades is obtained by differentiating Equation (3.1) with respect to time. Therefore,

$$\left. \begin{aligned} v_x &= \frac{dx}{dt} = V_f \mp R\omega \sin \omega t = V_f \mp V_{cir} \sin \omega t \\ v_y &= \frac{dy}{dt} = -R\omega \cos \omega t = -V_{cir} \cos \omega t \end{aligned} \right\} \dots (3.4)$$

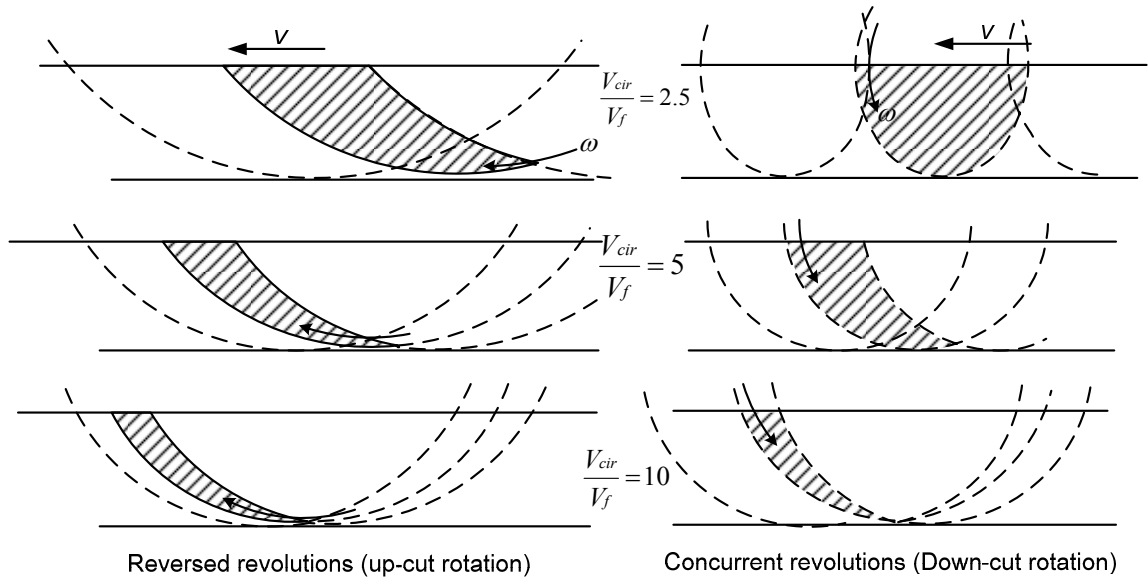


**Figure 3.3:** Shapes of slices for down-cut and up-cut rotation as a function of the ratio of the peripheral speed to forward speed.  $R\omega/V_f = \lambda$ . Number of blades operating in one plane  $z = 3$  (Bernacki *et al.*, 1972)

The modulus of the absolute velocity,  $V_a$ , of the rotor blade tip (Sineokov & Panov, 1978) is given by:

$$V_a = \sqrt{V_x^2 + V_y^2} = \sqrt{V_f^2 \pm 2V_fV_{cir} \sin \omega t + V_{cir}^2} \quad \dots (3.5)$$

Inserting  $\lambda$  and  $\alpha = \omega \cdot t$  into Equation (3.5) gives,

$$V_a = V_f \sqrt{\lambda^2 \pm 2\lambda \sin \alpha + 1} \quad \dots (3.6)$$

Equation (3.6) shows that the absolute velocity of the rotor blade tip is variable and is influenced by the angle of rotation of the blade in relative motion. The tilling speed is directed along the tangent to the absolute trajectory of motion of the blade (Sineokov & Panov, 1978; Meriam & Kraige, 1987).

### 3.2.2 The bite length

The bite length or blade delivery is determined by considering the process of soil cutting by two adjacent blades in one vertical plane and mounted on the same side of the flange (Figure 3.4).

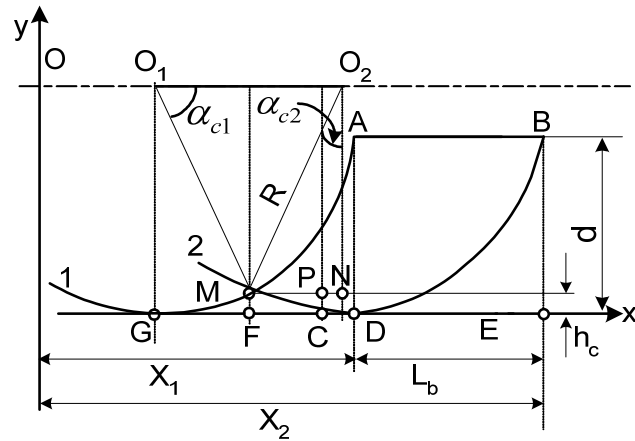


**Figure 3.4:** Determination of the bite length and the undisturbed peak crest heights (Sineokov & Panov, 1978)

With reference to Figure 3.4, the trajectory of Blade 1 is displaced with respect to that of the adjacent Blade 2 along the horizontal line through a certain value,  $L_b$ , called the bite length (Sineokov & Panov, 1978). The value of  $L_b$  is given by:

$$L_b = V_f t_b \quad \dots (3.7)$$

where:

$t_b$  = time during which the blades rotate through an angle, equal to the angle between the adjacent blades on the same side of a flange (s).

If the number of blades in one plane of rotor flange is  $z$ , then the angle between adjacent blades, in radians, is equal to  $\frac{2\pi}{z}$ . In such a case, the time  $t_b$  is given by

$t_b = \frac{2\pi}{z\omega}$  and the bite length,  $L_b$  is expressed as:

$$L_b = \frac{2\pi V_f}{z\omega} \text{ or } L_b = \frac{2\pi R}{\lambda z} \quad \dots (3.8)$$

Equation (3.8) shows that the bite length is a constant quantity that is dependent on the rotavator radius,  $R$ , the number of blades on the same side of a flange,  $z$  and the kinematic parameter,  $\lambda$ . The value of the bite length is one of the principal technological parameters of rotavators (Chamen *et al.*, 1979) and determines the degree of chopping of the processed soil (Sineokov & Panov, 1978).

### 3.2.3 Furrow bottoms produced by rotavators

During tillage operations, rotavators produce furrow bottoms with peaks of undisturbed (untilled) soil (Figure 3.4). These undisturbed peaks are dependent on the direction of rotation and the ratio of the peripheral to the forward travel speed. The non-uniformity of the furrow bottoms can be excessive and be agronomically undesirable. Therefore, in the design of rotavators, selection of parameters that will ensure the occurrence of minimum height of undisturbed peaks, are important.

In developing the expression for the determination of the peak crescent height,  $h_c$ , many researchers (Sineokov & Panov, 1978; Bosoi *et al.*, 1988; Hendrick & Gill, 1976) considered paths of adjacent tiller blades revolving in one vertical plane (Figure 3.4). The height of peaks,  $h_c$  is equal to the ordinate of point M, which is the point of intersection of two adjacent cycloids. This peak height is given by:

$$h_c = R(1 - \sin \alpha_c) \quad \dots (3.9)$$

The angle of rotation of the tiller radius that corresponds to maximum peak height of the crests formed first (Blade 1) is:

$$\alpha_{c_1} = \sin^{-1} \left( 1 - \frac{h_c}{R} \right) \quad \dots (3.10)$$

where:

$\alpha_{c_1}$  = the angle the first blade makes with the maximum crest height (rad.)

The angle of rotation (Figure 3.4) of the adjacent blade (Blade 2) corresponding to the point of intersection of the cycloids (M), which give the peak height at the bottom of the furrow, is given by (Sineokov & Panov, 1978)

$$\alpha_{c_2} = \frac{2\pi}{z} + \pi - 2\alpha_{c_1} \quad \dots (3.11)$$

where:

$\alpha_{c_2}$  = the angle at the second blade make with the maximum crest height (rad.).

$\frac{2\pi}{z}$  = the angle between any two adjacent blades on a flange on the rotor (rad.)

$z$  = the number of blades in the same vertical plane.

By the time the adjacent blade (Blade 2) reaches the point of intersection, M, the centre of the rotor will have moved a horizontal distance equal to  $\overline{O_1O_2}$ . This distance is equal to  $V_f t$ , which is equal to the bite length (or blade delivery)  $L_b$ . Since  $t = \alpha/\omega$ , where  $\alpha$  is the angle turned at  $\omega$  rad/s in time  $t$ , the distance  $\overline{O_1O_2}$  may be expressed as:

$$\overline{O_1O_2} = V_f t = V_f \left( \frac{2\pi}{z\omega} + \frac{\pi - 2\alpha_{c1}}{\omega} \right) \quad \dots (3.12)$$

The same distance  $\overline{O_1O_2}$  may be expressed in terms of the rotor radius as:

$$\overline{O_1O_2} = 2R \cos \alpha_{c1} \quad \dots (3.13)$$

Since Equation (3.12) and Equation (3.13) represent the same point, and because  $\cos \alpha_{c1} = \sqrt{1 - \sin^2 \alpha_{c1}}$ , it follows that Equation (3.13) may be expressed as:

$$2R \sqrt{1 - \sin^2 \alpha_{c1}} = \frac{V_f}{\omega} \left( \frac{2\pi}{z} + \pi - 2\alpha_{c1} \right) \quad \dots (3.14)$$

Given that  $\alpha_{cr} = \sin^{-1}(1 - h_c/R)$  and since for small values of  $\alpha_{c1}$ ,  $\sin \alpha_{c1} \approx \alpha_{c1}$ , with acceptable levels of accuracy. Also recalling that  $R\omega = V_{cir}$  and  $V_{cir}/V_f = \lambda$ , after substituting these values in Equation (3.14) and making the necessary transformations (Sineokov & Panov, 1978), results in Equation (3.15).

$$\lambda = \frac{\left( \frac{\pi}{z} \pm \frac{\pi}{2} \right) \mp \sin^{-1} \left( 1 - \frac{h_c}{R} \right)}{\sqrt{2 \frac{h_c}{R} - \frac{h_c^2}{R^2}}} \quad \dots (3.15)$$

The  $\pm$  and  $\mp$  in Equation (3.15) takes care of the direction of rotation of the rotor. Equation (3.15) combines the rotavator principal parameters  $\lambda$ ,  $R$  and  $z$ , with the peak crest height,  $h_c$ .

The relations given above, do not permit easy manual determination of the absolute peak crest height,  $h_c$  (Sineokov & Panov, 1978), and the use of the geometric relations in Figure 3.4 is recommended for the determination of the absolute value of the peak height of the crest,  $h_c$ , by considering the path of the points on adjacent loci (Hendrick &



Gill, 1976) to have a rolling radius equal to  $\frac{V_f}{\omega} = \frac{R}{\lambda}$ . Using this approach, the angle between the rotor radius, drawn from  $O_2$  to the point M, and the vertical in Figure 3.4 is denoted as  $\alpha_{c2}$ . This angle, from the triangle  $O_2MN$ , can be expressed as,

$$\sin \alpha_{c2} = \frac{\overline{MP} + \overline{PN}}{R}$$

From symmetry of the position of the crest in Figure 3.4 with respect to the two adjacent cycloids,  $\overline{MP} = \frac{L_b}{2}$ , where  $L_b$  is the bite length or the blade delivery.

The length  $\overline{PN}$  (Sineokov & Panov, 1978) is given by:

$$\overline{PN} = \frac{V_f}{\omega} \alpha_{c2} = \frac{R}{\lambda} \alpha_{c2}$$

The value of  $\sin \alpha_{c2}$  can therefore be expressed as:

$$\sin \alpha_{c2} = \frac{\frac{L_b}{2} + \frac{R}{\lambda} \alpha_{c2}}{R} \quad \dots (3.16)$$

Putting  $\sin \alpha_c = \alpha_c$  for small angles, and making the necessary transformation gives:

$$\alpha_{c2} = \frac{\pi}{z(\lambda - 1)}.$$

Hence the crest height is given by:

$$h_c = R \left[ 1 - \cos \left( \frac{\pi}{z(\lambda - 1)} \right) \right] \quad \dots (3.17)$$

If the maximum peak crest height,  $h_c$  is dictated by agronomic requirements, the kinematic parameter  $\lambda$  can be calculated from:

$$\lambda = \frac{\pi}{z \cos^{-1} \left( 1 - \frac{h_c}{R} \right)} \pm 1 \quad \dots (3.18)$$

The crest-shaped nature of the furrow bottoms produced by rotavators is one of the tiller's important indices of performance. The height of ridges can be used as means of determining the effective tilling depth of rotavators (Hendrick & Gill, 1976), even though the exact agronomic significance of the peak crest height has not been investigated.

In practice, the peak crest height,  $h_c$ , may be less than the theoretically determined  $h_c$  using Equation (3.17), due to crumbling away or breaking loose of the untilled soil, though it is uncut by the rotor blade (Sineokov & Panov, 1978). The actual crest height may therefore be approximately given by:

$$h_{ac} = \frac{h_c}{k_c} \quad \dots (3.19)$$

In Equation (3.19),  $k_c$  is the coefficient allowing for reduction of the crest height due to breakage of the peak crest height as the tillage operation progresses. Values of  $k_c$  depend on the soil type, and average  $k_c$  values have been given by Sineokov and Panov (1978) as 2.0 for sandy loam, 1.5 saturated sandy-loams and 1.0 for heavy sandy-loam.

### 3.2.4 Side surface area of the soil chip

The soil chip cut by the blades of rotavators is best looked at in terms of the area of the side surface, thickness, and the volume. The three constitute the chips of soil slices cut by rotavator blades.

Based on the geometric relation of Figure 3.4, the area of the surface ABM can approximately be given as:

$$A_{ABM} = L_b d \quad \dots (3.20)$$

The crest area,  $A_{cr}$ , which is the area under GMC (Figure 3.4), must be taken into consideration, for accurate determination of the side surface area. Using the equality of the areas under BEC and ADG, the side surface area,  $A_{AMB}$  is given as:

$$A_{ABM} = A_{ABCG} - A_{cr} = L_b d - A_{cr} \quad \dots (3.21)$$

The crest area,  $A_{cr}$  is equal to twice the area under CFM. This area is equal to half the crest area and can be determined from:

$$A_{CFM} = \int_{t_1}^{t_2} yx dt = \int_{t_1}^{t_2} R(1 - \sin \omega t)(V_f - V_{cir} \sin \omega t) dt \quad \dots (3.22)$$

where:

$t_1$  = time taken by the leading blade to turn through angle  $\alpha_{c1}$

$t_2$  = time taken by the second blade to turn through angle  $\alpha_{c2}$

Changing the limits of integration and noting that  $t = \frac{\alpha}{\omega}$ , and that  $dt = \frac{d\alpha}{\omega}$ ,  $A_{CFM}$  can be expressed as:

$$A_{CFM} = \int_{\alpha_1}^{\alpha_2} R(1 - \sin \alpha)(V_f - V_{cir} \sin \alpha) \frac{d\alpha}{\omega} \quad \dots (3.23)$$

Integrating Equation (3.23) and taking limits of integration as  $\alpha_1 = \pi/2$  and  $\alpha_2 = \alpha_c$  gives

$$A_{CFM} = \frac{R^2}{\lambda} \left( -\frac{\pi}{2} + \alpha_c + \cos \alpha_c \right) + R^2 \left( \cos \alpha_c - \frac{\pi}{4} + \frac{\alpha_c}{2} - \frac{1}{4} \sin 2\alpha_c \right) \quad \dots (3.24)$$

The angle  $\alpha_c$  (Figure 3.4) is obtained from the expression  $\alpha_c = \frac{\pi}{2} - \alpha_{c1} = \frac{\pi}{2} - \frac{\pi}{z(\lambda - 1)}$ .

### 3.2.5 Chip thickness

The thickness of the soil cut by blades of a rotavator varies continuously from a maximum value to zero for a down-cut rotating rotor, and from a minimum (zero) to a maximum for an up-cut rotating rotor. The chip thickness must be known when calculating the tilling power of rotary blades. In general many methods, based on geometry of the cut soil slice have been presented for approximately determining the thickness of the chip (Sineokov & Panov, 1978).

In the first approximation approach (Sineokov & Panov, 1978), the thickness is the distance between two adjacent trajectories, measured in the radial direction from the centre of the rotor (Figure 3.6). In this case; the thickness  $\mathcal{G}$  is expressed as,

$$\mathcal{G} = L_b \cos \alpha \quad \dots (3.25)$$

where:

$L_b$  = is the bite length

$\alpha$  = the angle of rotation of the blade.

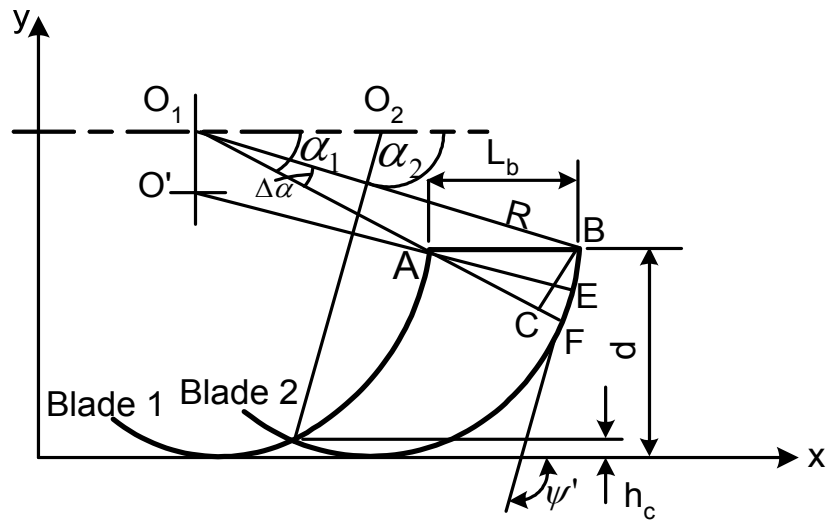


**Figure 3.6:** An illustration for determination of the soil chip thickness (Sineokov & Panov, 1978)

The maximum sizes of the chip thickness in this case comprise the angle  $\alpha = \alpha_1$ , i.e. the angle turned through at the beginning of blade tilling and is calculated (Sineokov & Panov, 1978) using:

$$g_{\max} = L_b \cos \alpha_1 = \frac{L_b}{R} \sqrt{2Rd - d^2} \quad \dots (3.26)$$

where:

$d$  = depth of tillage

$g_{\max}$  = equal to the length  $\overline{AE}$

Equation (3.26) underestimates the value of maximum thickness of the soil chip by a value equal to the length  $\overline{CF}$  (Figure 3.6). Secondly, the equation is only applicable for kinematic parameter ( $\lambda$ ) values in excess of 10, when the tilling trajectory of the blades is almost circular (Sineokov & Panov, 1978). For such high values of  $\lambda$ , the rotational velocity for most rotary tillage operations is too high and is associated with high power expenditure, accompanied with excessive pulverisation of the tilled soil, both of which, are undesirable.

The second approximation was presented by Kaneve (as cited in Sineokov & Panov, 1978). In this method, the section CF is taken into consideration and gives the soil thickness as:

$$g = L_b \cos \alpha + R(1 - \cos \Delta\alpha) \quad \dots (3.27)$$

where:

$$\Delta\alpha = \sin^{-1} \left( \frac{L_b \sin \alpha}{R} \right) \text{ (see Figure 3.6)}$$

The third method (Sineokov & Panov, 1978), which is more accurate, is based on the geometry of Figure 3.6. In this latter approach, the thickness of the soil chip is obtained by measuring the section  $\overline{AE}$  as a straight line, drawn from the instantaneous centre of the rotor O, i.e. along the normal to the external cycloid.

The thickness,  $g$  of the chip is then given by:

$$g = L_b \sin \psi' \quad \dots (3.28)$$

where:

$\psi'$  = the angle formed by the positive direction of the tangent at the given point of the cycloid and the positive direction of the abscissa.

The angle  $\psi'$  (Sineokov & Panov, 1978) is obtained from:

$$\tan \psi' = \frac{dy}{dx} = \frac{-V_f \cos \alpha}{V_{cir} \mp V_f \sin \alpha} \quad \dots (3.29)$$

From Equation (3.29) the angle  $\psi'$  may be expressed as:

$$\psi' = -\tan^{-1} \left( \frac{\lambda \cos \alpha}{1 \mp \lambda \sin \alpha} \right) \quad \dots (3.30)$$

Substituting  $\psi'$  into Equation (3.28) gives the soil chip thickness,  $g$ , as:

$$g = L_b \sin \left( -\tan^{-1} \left( \frac{\lambda \cos \alpha}{1 \mp \lambda \sin \alpha} \right) \right) \quad \dots (3.31)$$

In some cases (Sineokov & Panov, 1978) it may be sufficient to use the concept of average thickness of the soil chip. In such an approach, the average thickness of the chip

is expressed as  $L_{bav} = L_b \cos \frac{\alpha_k}{2}$ , where  $\alpha_k = \alpha_2 - \alpha_1$ . The angle,  $\alpha_k$ , being the difference between the angles turned through by the blade at the beginning and the end of the soil cutting process. Expressing the angles  $\alpha_1$  and  $\alpha_2$  in terms of depth of tillage,  $d$ , and the peak crest height,  $h_c$ , (Sineokov & Panov, 1978) gives the average cut soil thickness as:

$$g_{av} = L_b \cos \frac{1}{2} \left[ \left( 1 - \frac{h_c}{R} \right) - \sin^{-1} \left( 1 - \frac{d}{R} \right) \right] \quad \dots (3.32)$$

### 3.2.6 Volume of the soil chip

Figure 3.7 shows the dimensions of a soil block chipped-off by a down-cut rotavator blade. The width of the chip,  $w$ , is the distance between adjacent blades along the rotor shaft axis. The volume of the chip can be approximately determined (Hendrick & Gill, 1971a; Sineokove & Panov, 1978) as:

$$V_{chip} = L_b dw \quad \dots (3.33)$$

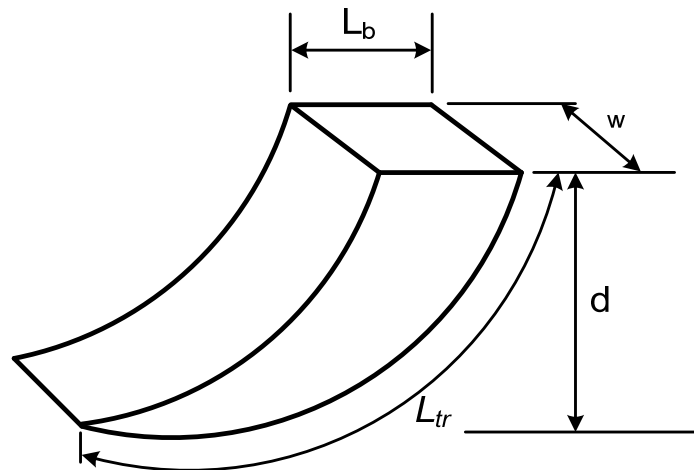


**Figure 3.7:** The main dimensions of a soil chip cut by a down-cutting rotary blade (Hendrick & Gill, 1971a)

For accurate determination of  $V_{chip}$ , it is necessary to take the volume of the crest into account (Figure 3.4). The volume of the crest is given by:

$$V_{crest} = A_{cr} w \quad \dots (3.34)$$

where:

$$A_{cr} = 2A_{CFM} \text{ (} A_{CFM} \text{ is given by Equation (3.24))}$$

Therefore the actual volume,  $V_{ac}$  of the soil is

$$V_{ac} = V_{chip} - V_{crest} \quad \dots (3.35)$$

### 3.2.7 Length of the tilling route

The length of the tilling route,  $L_{tr}$ , (Figures 3.7) is the length of the cycloid section from the point of intersection of the blade trajectory with the soil surface to the point of intersection of two adjacent trajectories at the maximum peak crest height (point M in Figure 3.4). An elemental arc of the trajectory is given by

$$dL_{tr} = \sqrt{dx^2 + dy^2} \quad \dots (3.36)$$

Substituting the values of the first derivative of the equation of motion (see Equation 3.3) of the rotor blade end point gives:

$$dL_{tr} = V_f \sqrt{1 \mp 2\lambda \sin \alpha t + \lambda^2} \quad \dots (3.37)$$

From Equation (3.37) the tilling route  $L_{tr}$  is given by:

$$L_{tr} = \int_{\omega t_1}^{\omega t_2} dL_{tr}$$

Changing limits of integration with respect to angle of rotation  $\alpha_i = (\omega \cdot t_1)$ ,  $\alpha_e = (\omega \cdot t_2)$

and  $dt = \frac{d\alpha}{\omega}$  gives the tilling route length as:

$$L_{tr} = R \int_{\alpha_i}^{\alpha_e} \sqrt{1 \mp 2\lambda \sin \alpha + \lambda^2} d\alpha \quad \dots (3.38)$$

Equation (3.38) can be expressed (Sineokov & Panov, 1978) as:

$$L_{tr} = \frac{R}{\lambda} \sqrt{1 + \lambda^2} \int_{\alpha_i}^{\alpha_e} \left( 1 \mp \frac{2\lambda \sin \alpha}{1 + \lambda} \right)^{\frac{1}{2}} d\alpha \quad \dots (3.39)$$

Integration of Equation (3.39) belongs to elliptic integrals (Sineokov & Panov, 1978) and can be evaluated using numerical methods. The approximate values of the integral can be obtained by expressing the function under integration in Taylor series form. For the first three terms (Walters & Owen, 1996), Equation (3.39) takes the form:

$$L_{tr} = R\sqrt{1+\lambda^2} \left[ (\alpha_e - \alpha_i) \mp \frac{\lambda}{1+\lambda^2} (\alpha_e^2 - \alpha_i^2) - \frac{\lambda^2}{6(1+\lambda^2)} (\alpha_e^3 - \alpha_i^3) \right] \quad \dots (3.40)$$

The angle  $\alpha_i$  correspond (Figure 3.8) to the beginning of blade cutting and is determined from the relation  $\alpha_i = \sin^{-1} \left( 1 - \frac{d}{R} \right)$  and the angle  $\alpha_e$ , correspond to the end of the soil cutting process by the blade.

The value of  $\alpha_e$  is obtained from Figure 3.8 as:

$$\alpha_e = \frac{\pi}{2} + \alpha_{ie} \quad \dots (3.41)$$

From the foregoing analysis, it is evident that the length of the tilling route depends on the rotor radius,  $R$ , the kinematic parameter,  $\lambda$ , tilling depth,  $d$ , number of cutting blades on the same side of a flange,  $z$ , and the direction of rotation (the  $\pm$  sign in Equation (3.40)).

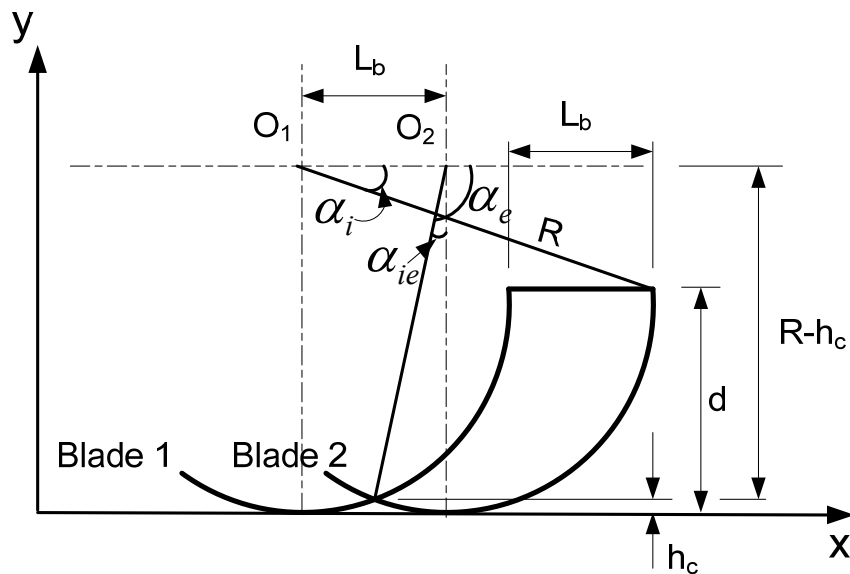


**Figure 3.8:** Determination of the start and end angles of soil cutting by a blade in a down-cut operation



### 3.3 Identification of torque requirement sources

The configuration and dimensional details of the blade used in this study is as shown in Figure 3.9.

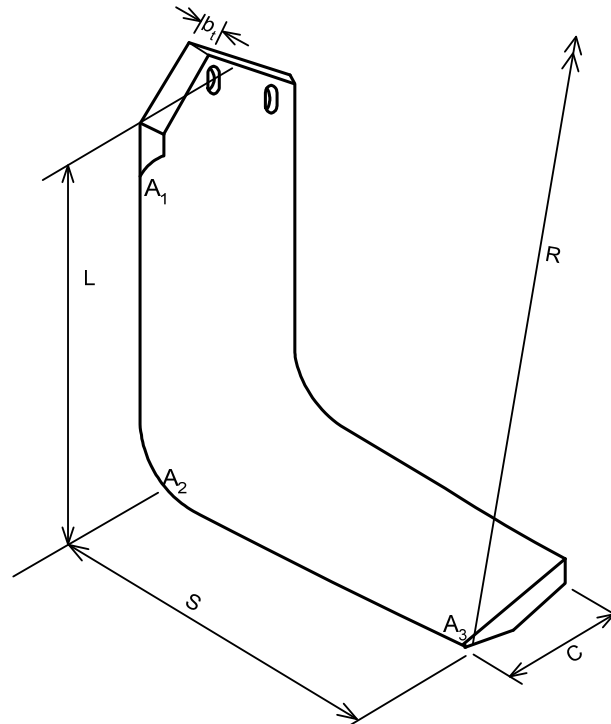
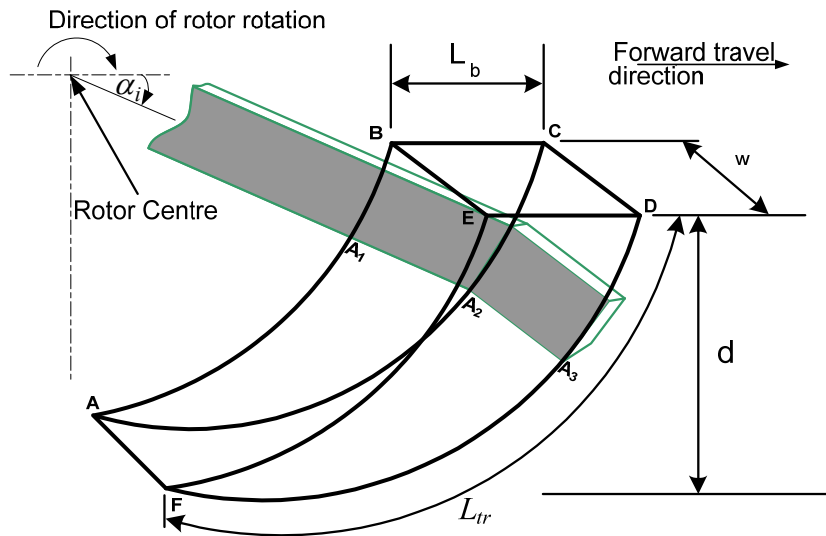


**Figure 3.9:** Line drawing of the standard ‘L-shaped’ blade ( $C$  – chord of the blade, 80 mm at tip and 100 mm at the L–S intersection;  $L$  – vertical section (stem or leg), 100 mm;  $S$  – horizontal section (span), 130 mm;  $b_t$  – thickness of the blade, 7 mm;  $R$  – radius of the rotor, 500 mm;  $\overline{A_1A_2}$  – cutting edge of the leg;  $\overline{A_2A_3}$  – leading edge of the leg)

A hypothetical soil-tool interaction of a down-cutting rotavator fitted with an L-shaped blade is shown in Figure 3.10, for a given depth of tillage and kinematic parameter,  $\lambda$ . The width of the soil slice ( $w$ ) corresponds to the span of the blade (Figure 3.9), and it was assumed that the face FEDF separated from the uncut soil body breaks away in a vertical manner.

For a down-cut direction of rotation at a given kinematic parameter  $\lambda$ , the length of cut,  $L_{tr}$  (Figure 3.10) is dependent on the set depth of tillage. The set depth of tillage determines the angle at which the cutting edge of the blade comes into contact with the soil surface and the angle at which the blade stops the soil cutting process.



**Key:**

- Face ABEF - Previously cut surface by the span of the preceding blade
- Face ABCA - Soil surface in being cut by the leg of the cutter
- Face ACDF - Soil surface cut by the blade of the cutter
- Face FEDF - Soil surface sheared from the un-cut soil body

**Figure 3.10:** The soil-tool interaction for a down-cutting rotavator fitted with an L-shaped blade ( $L_{tr}$  = length of cut;  $w$  = width of the blade;  $d$  = depth of tillage;  $L_b$  = bite length)

### 3.4 Proposed analytical model for rotavator torque requirements

In processing the soil using the standard L-shaped blade, two of its distinct parts come into contact with the soil, viz., the vertical section (also called the leg or stem), and the horizontal section (also called span). In terms of torque requirements, the stem requires torque for cutting and separating the cut soil slice along face ABCA (Figure 3.10), and for overcoming the soil-metal friction on the backside of the leg in contact with the uncut soil mass body. The span requires torque for overcoming soil shear strength, soil-metal friction (on the inside), cutting by the leading edge, and the acceleration and throwing of the cut soil slice.

The proposed analytical model in this section is based on forces that need to be overcome by the L-shaped blade when cutting the soil. From the blade configuration and its interaction with the soil (Figure 3.9 and Figure 3.10), torque is required to overcome the following soil and soil-tool interaction forces:

- soil-metal friction on the backside of the leg in contact with uncut soil body

- soil forces due to the soil-tool interaction by the span of the blade
- penetration resistance of the cutting edge of the span from the time the blades comes into contact with the soil to the time the cutting action ends (Figure 3.10).

### 3.4.1 Length of the blade in contact with the soil

The first parameter calculated in order to derive an expression for the torque requirement due to the soil-metal friction by the leg of the blade was the length of the leg in contact with the un-cut soil mass at different instantaneous tillage depths for a single blade. This is because in rotary tillage the length of the leg of the blade in contact with the soil varies from zero (before the blade enters the soil body) to a maximum value equal to the set depth of tillage after the blade has turned through an angle  $\alpha = \pi/2$  from the horizontal (Figure 3.11). At this latter angle, the blade is vertical and the length in contact with soil is equal to the set tillage depth.

The length of the leg of the blade in contact with the soil was calculated by first, determining the co-ordinates of the tip of the cutting edge of the span,  $(x_i, y_i)$  at the at different instantaneous time moments. The coordinates of the tip of the blade for a down-cutting rotavator was obtained by modifying Equation (3.1). The modified expression takes the form:

$$\left. \begin{aligned} x_i &= V_f t_i + R \cos \alpha_i = V_f t_i + R \cos(\omega t_i) \\ y_i &= R(1 - \sin \alpha_i) = R(1 - \sin(\omega t_i)) \end{aligned} \right\} i=1, 2, 3, \dots, n \quad \dots (3.42)$$

where:

$i$  = position of the blade along the cutting path of the blade

$\alpha_i$  = the angle the blade turns through in time,  $t_i$  (rads)

$t_i$  = time of rotation of the blade though angle,  $\alpha_i$ , from the horizontal(sec.)

From the coordinates of instantaneous depth along the cutting path of a blade, the length of the leg of the blade in contact with the soil is obtained from the geometric relations (Figure 3.11). The length of the blade in contact with the soil in Figure (3.11) at point  $P_i$  is obtained by using the geometric relation as follows:

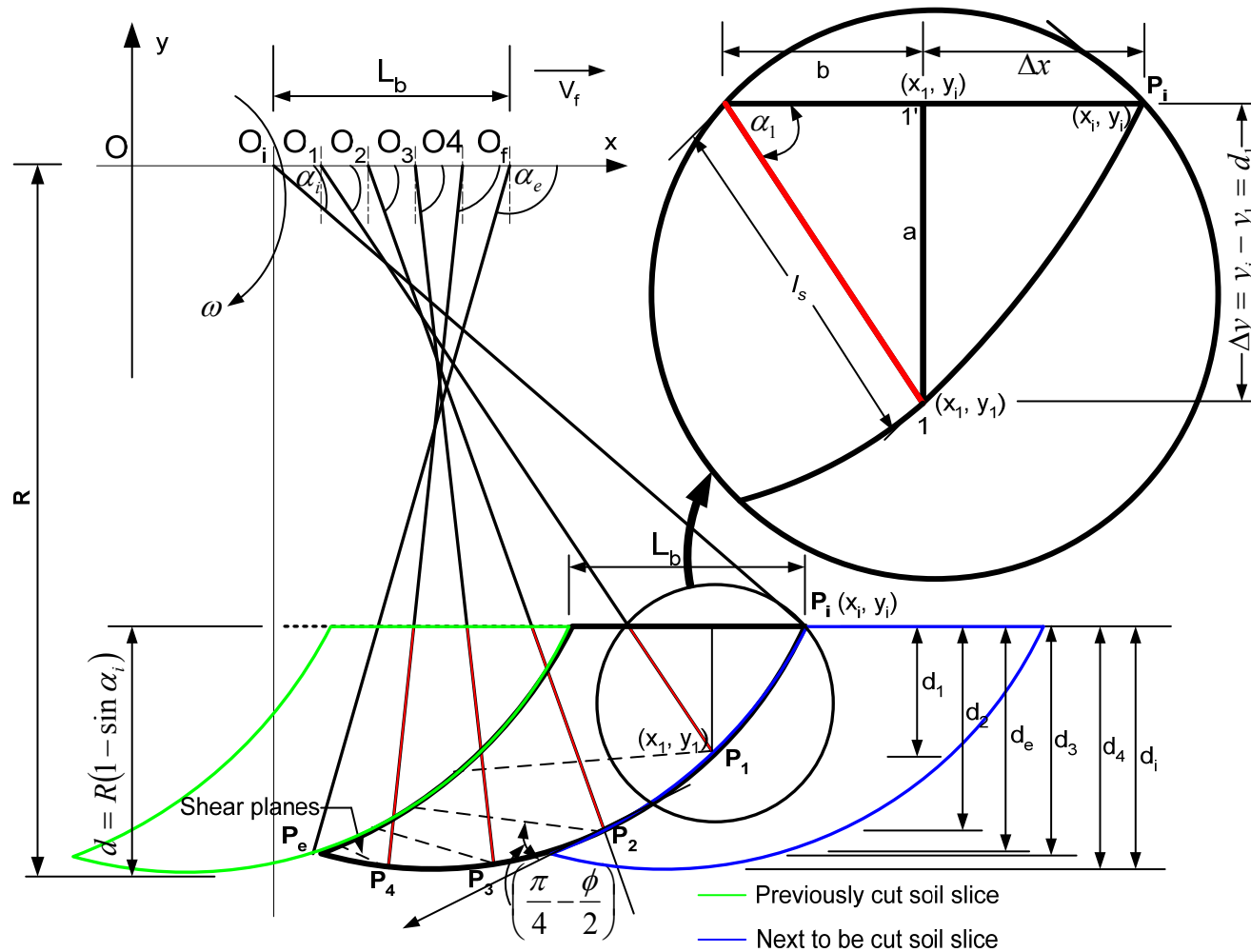


**Figure 3.11:** Theoretical shear planes in a soil slice at different positions for a down-cutting blade:  $\alpha_i$  – the angle at which the blade comes into contact with the ground surface and starts cutting the soil;  $\alpha_e$  – angle at which the cutting edge of blades exits the soil; 1; 2; 3; 4 ...,  $n$  – the position of the blade at various positions where shear planes are assumed to occur

1. Determine the coordinates  $(x_i, y_i)$ , of the point at which the blades comes into contact with the horizontal ground surface
2. Allow the blade to advance to a second point along the cutting path, say position 1, in time  $t_1 = \frac{\alpha_1}{\omega}$ . Determine the coordinates of the blade at this new location. In this case  $t_1$  is the time required to move from point  $i$  to point 1 at a constant rotor speed,  $\omega$ .
3. The depth of the blade at the new location  $d$  is given by:

$$d_1 = \Delta y = y_i - y_1 \quad \dots (3.43)$$

4. The length of the blade in contact with the soil (see Figure 3.4, magnified part) is then obtained as:

$$l_s = \frac{\Delta y}{\sin \alpha_1} = \frac{d_1}{\sin \alpha_1} \quad \dots (3.44)$$

The above procedure was then repeated for all the locations of interest of the cutting edge of the blade, at pre-determined time intervals, and the length of the backside of the leg of the blade in contact with the uncut vertical soil mass determined. A similar expression was used for the other positions of the tip of the cutting end of the span.

### 3.4.2 Torque requirements due to the span of the blade

From Figure 3.10, torque is required by the span of the L-shaped blade for the following:

- Accelerating the cut soil by the span of the blade
- Overcoming the soil-metal friction and adhesion on the span of the blade
- Overcoming the soil-soil friction on the shear plane
- The continuous penetration resistance by the tip (cutting edge) of the span in the form of the tip reaction.

The first step in development of the mathematical model for torque requirements for the span was to make a number of assumptions. The first assumption made was that during an instantaneous time movement, the span of an L-shaped blade behaves like an inclined passive tillage blade. Secondly, given that the width of the span of the blade is greater than its depth (Figure 3.9), its instantaneous moment in time behaviour when

processing the soil is analogous to that of a wide blade. This wide blade consideration implies that the 'end effect' which has considerable influence on the soil-tool interaction forces for narrow tillage passive tools is negligible and can be ignored. The third assumption was that the heaving of soil in front of the tool was negligible, and was also ignored in the resultant failed soil wedge. With these assumptions, the assumed shape of the soil failure wedge by the span at an instantaneous time moment is as shown in Figure 3.12.

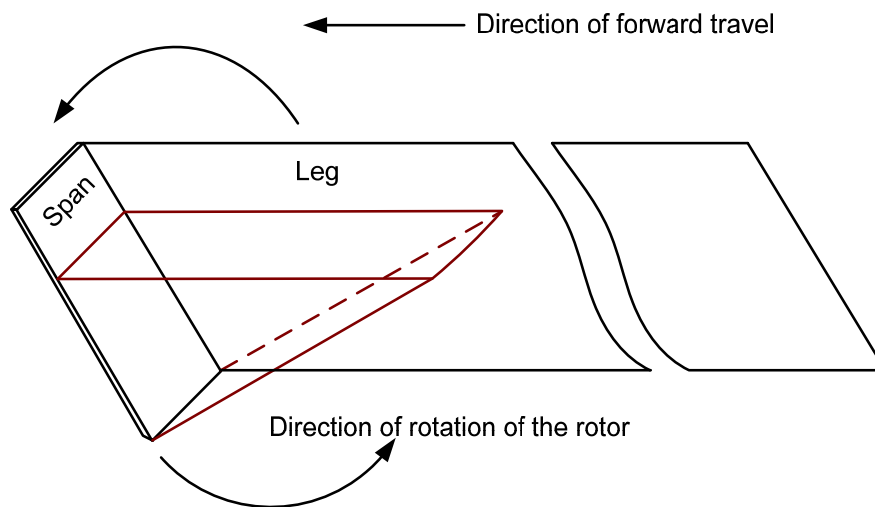


**Figure 3.12:** The assumed instantaneous time moment soil failure wedge in front the span

The next step was the identification of the soil-tool interaction forces on the different planes that would enable the development of a soil-tool interaction forces model that would enable the prediction of torque requirements. In this regard, 3-D soil failure approach was chosen. Three dimensional analytical resistance models are better suited to explain soil resistance induced by separation-mechanism of inclined tillage blades. This is because the 3-D resistance models predict soil resistance reasonably well by analytically representing forces involved in the soil-tool interaction with 3-dimensional soil failure geometries whereas 2-D analytical models and the empirical models are unable to do this.

Among the 3-D resistance models, Perumpal-Desai-Grisso model (Perumpal, Grisso & Desai, 1983) based on the limit equilibrium analysis was chosen in this study as the basic

model, from which soil-tool interaction forces for the span was developed. The torque requirements were to be derived from the force prediction model by determining the distance of the point of action of the resultant force to the centre of the rotor. This 3–D analytical model was appropriate in this case as:

- it allows a relatively simple soil failure shape without relying on experimental results; and
- its proposed failure shape is close to the one created by the span of the L-shaped blade (Figure 3.13) used in this study as shown in the right side of Figure 3.13(b), which also shows the failure geometry of McKyes model (McKyes 1985) for comparison. The confinement of the soil wedge supported by the span by the leg of the L-shaped blade (Figure 3.12), and span being a ‘wide blade’ (Koolen & Kuipers, 1983) makes the Perumpral-Desai-Grisso model soil failure shape an appropriate approximation of the soil failure shape for the span at instantaneous time moments. An idealised soil failure wedge within the soil slice cut by a down–cutting rotavator is presented in Figure 3.14.

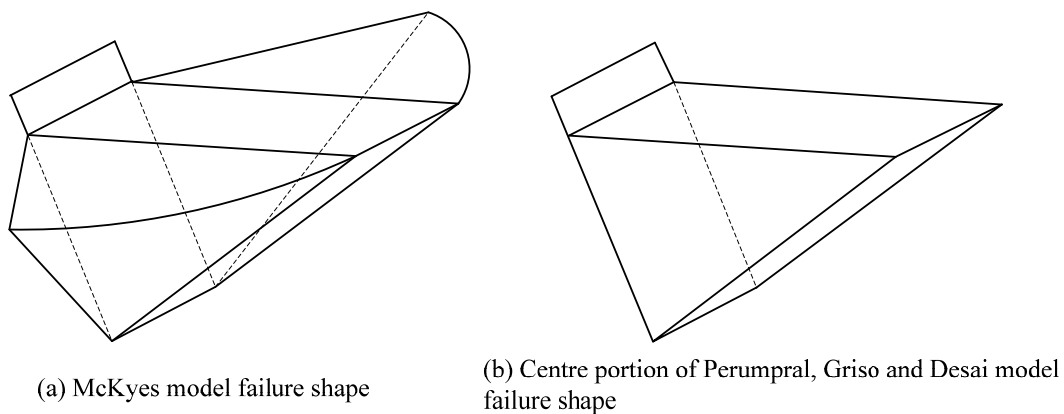


**Figure 3.13:** Outlines of soil failure shapes of McKyes and Perumpral-Grisso-Desai models for inclined blades

However, Perumpral-Desai-Grisso model needed to be modified and expanded such that it could predict the dynamic soil-tool interaction forces for a ‘wide blade’ moving in a trochoidal path with a non-uniform resultant velocity. The proposed model also needed to incorporate the L-shaped blade configuration, specifically the inclusion of the leg since

the Perumpral-Desai-Grisso model is based on an inclined rectangular plate without sides, such as the leg part of the L-shaped blade. Further modifications of this static model were also necessary to account for the dynamic nature of the soil-tool interaction in rotavator tillage. To this end, the centre wedge of Swick-Perumpral model for predicting the soil-tool interaction (Swick & Perumpral, 1988) was used to introduce the terms that accounted for the acceleration force. The centre wedge of the Swick-Perumpral model resembles the assumed idealised soil failure shape (Figure 3.14 and Figure 3.15) supported by the span of the L-shaped blade.

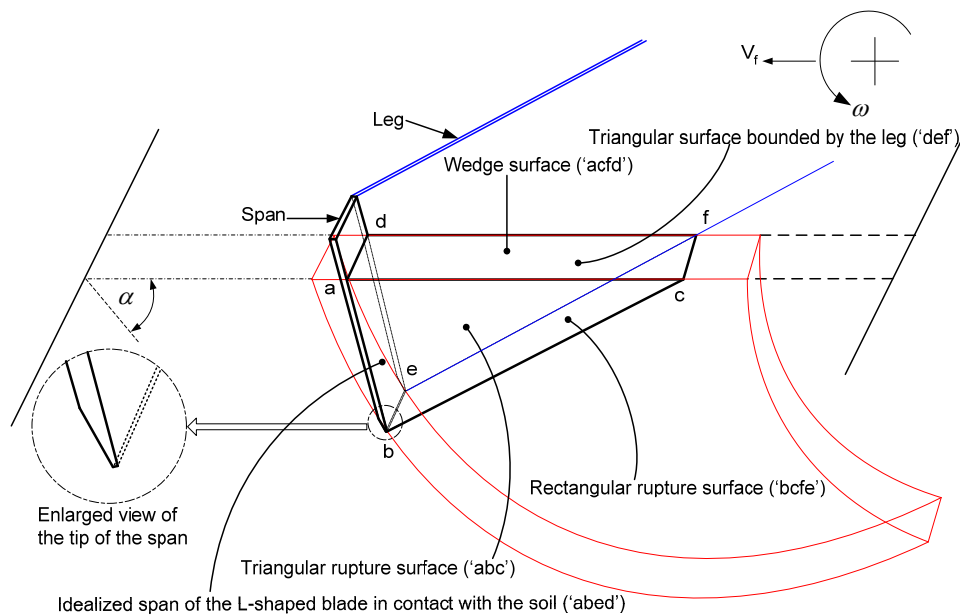


**Figure 3.14:** Geometric boundaries of the idealised separation failure wedge within the soil slice cut by the span of an L-shaped blade at an instantaneous depth for a down-cutting blade

Based upon the soil failure wedge, all the forces acting on the different surfaces are identified as shown in Figure 3.15. These forces contribute to the total force due to the wedge, designated as  $P_s$ ; which act at an angle  $\delta$ , normal to the surface of the span. The description of the all identified force components, per wedge surface, is as follows:

- Rectangular surface abed:
  - Adhesion force,  $F_{ad}$  due to adhesion between the span and the soil



- Soil-metal friction force on the interface between the soil and the span of the blade
- The force exerted on the span by the tool in the instantaneous direction of movement,  $P_s$
- Triangular surface abc:
  - Equal and opposite reaction normal forces,  $R$
  - Cohesion force,  $CF_2$  due to soil cohesion between the soil particles.
  - Friction force,  $SF_2$ , between soil particles, i.e., soil-soil friction

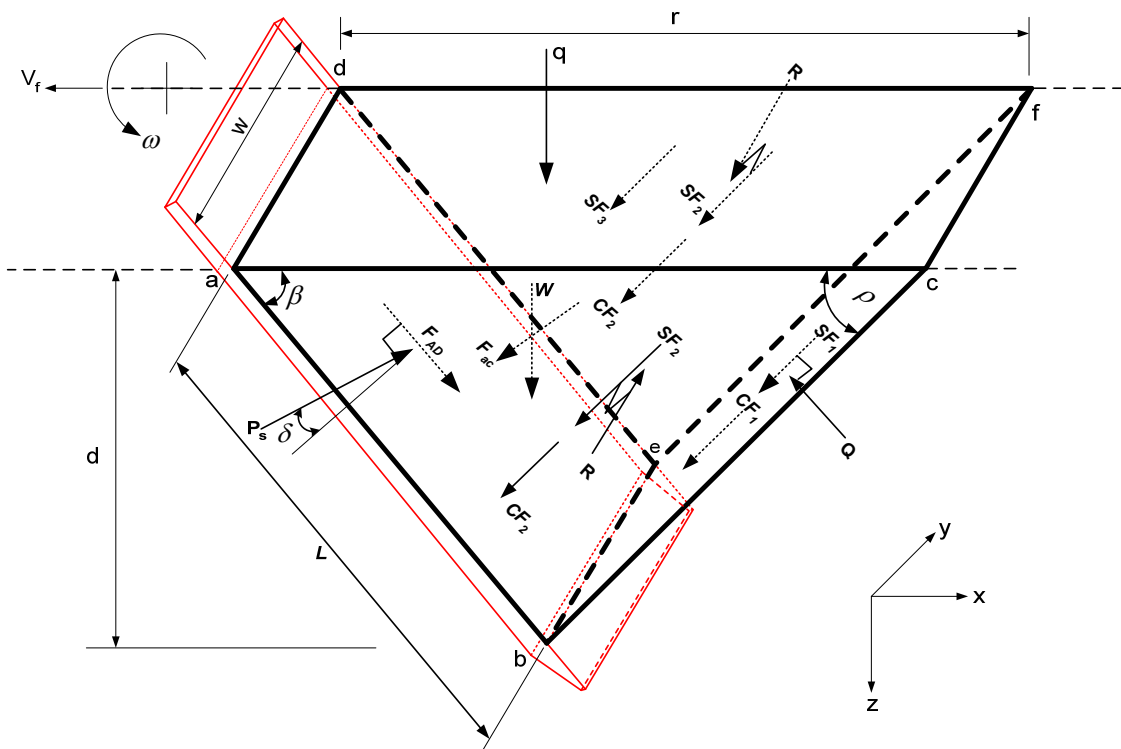


**Figure 3.15:** Breakdown of the soil-tool interaction forces on an idealised soil wedge for the span at an instantaneous time moment for a down-cutting rotavator tillage operation

- Rectangular rupture surface bcfe:
  - The normal acting force,  $Q$
  - Cohesion force,  $CF_1$  due to cohesion between soil particles
  - Friction force,  $SF_1$  due soil-soil friction between the soil particles on this plane

- Triangular surface def:
  - Equal and opposite reaction normal forces, R
  - Cohesion force,  $CF_2$  due to soil cohesion between the soil particles
  - Friction force,  $SF_3$ , due to soil-metal friction between the leg and the soil

Other additional forces identified due to the failed soil wedge were:

- Acceleration force  $F_{ac}$ ; a body force resisting the acceleration of the wedge
- Gravitational force,  $W$ , due to the weight of the wedge
- Surcharge force,  $F_q$ , due to the heaving of the soil in front of the span.

The angles used in Figure 3.15 are as defined below:

$\beta$ : angle that the tool makes with the horizontal during an instantaneous time moment (degrees). This is also called the rake angle.

$\rho$ : angle that the rupture surface makes with the horizontal (degrees)

$\delta$ : soil-metal friction angle (degrees)

$\phi$ : soil internal friction angle (degrees)

In order to include the contribution of the leg to the resistance in the soil separation process, a soil-metal friction force ( $SF_3$ ) on the triangular failure surface 'def' has been included. This is different from Perumpral-Desai-Grisso model, which includes only the cohesion force on the triangular surfaces 'abc' and 'def'. The inclusion of this force eliminates the need to separately include the leg part of the L-shaped blade (Figure 3.12) in the instantaneous idealised soil failure shape, as shown in Figure 3.15. Owing to the dynamic nature of the rotavator tillage, additional forces for the acceleration and the weight of the soil wedge have also been included.

### ***Calculation of the each force component***

With the exception of the acceleration force component, the calculation of the identified force components for the span is described below. The calculations are based on the 2-D drawing of the idealized soil failure wedge (Figure 3.16).

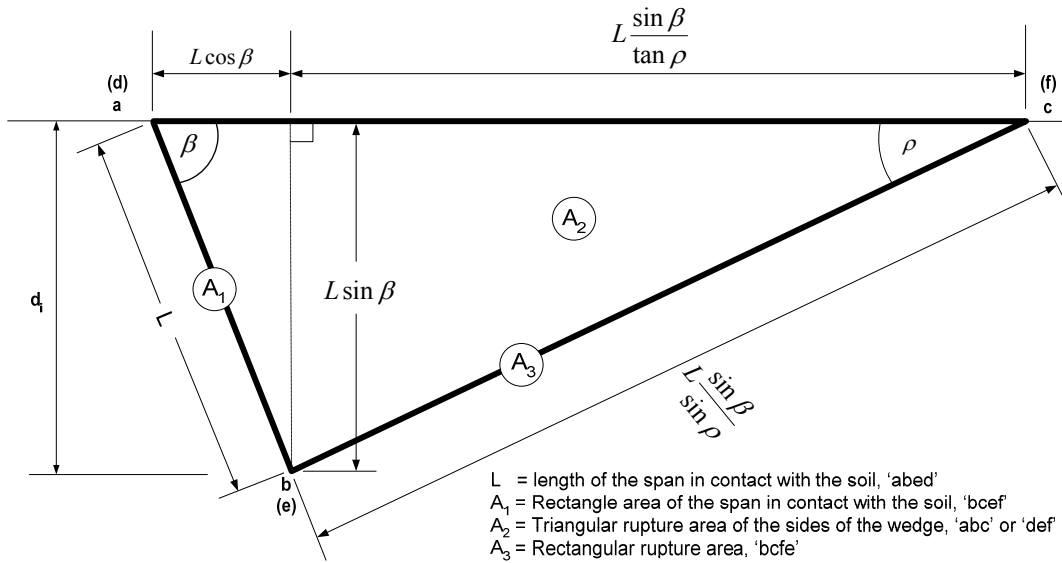


**Figure 3.16:** Dimensions of the soil failure wedge for calculating the force components

The expressions for the respective forces were obtained as:

- *The adhesion force.* The force of adhesion on the surface,  $F_{ad}$ , resisting the movement of the wedge on the span is given by:

$$F_{ad} = C_a \times A_1 = C_a \times w \times L$$

where:

$C_a =$  soil metal adhesion factor (kN/m<sup>2</sup>)

$A_1 =$  area of the span in contact with the soil, 'abcd' (m<sup>2</sup>)

$L =$  length of the span in contact with the soil (m)

- *Weight of the soil wedge.* The expression for weight of the failed soil wedge,  $W$ , obtained as:

$$\begin{aligned}
 W &= \gamma \times w \times A_2 \\
 &= \gamma \times w \times \frac{1}{2} \times (L \times \sin \beta) \times \left( L \times \cos \beta + \frac{L \times \sin \beta}{\tan \rho} \right) \quad \dots (3.47) \\
 &= \frac{1}{2} \times \gamma \times w \times L^2 \times \sin \beta \times \left( \cos \beta + \frac{\sin \beta}{\tan \rho} \right)
 \end{aligned}$$

where:

$\gamma =$  unit weight of the soil (kN/m<sup>3</sup>)

$A_2 =$  area of the triangular rupture surface, abc or def (m<sup>2</sup>)

- Cohesion force acting on rectangular failure surface *bcfe*. This was calculated as:

$$CF_1 = C_c \times A_3 = C_c \times w \times \left( L \frac{\sin \beta}{\sin \rho} \right) \quad \dots (3.48)$$

where:

$C_c$ = soil cohesion (kN/m<sup>2</sup>)

$A_3$ = areas of the rectangular rupture surface *bcfe* (m<sup>2</sup>)

- The soil-soil friction force was calculated as:

$$SF_1 = Q \tan \phi \quad \dots (3.49)$$

- The combined soil-metal friction force on the triangular surface *def*,  $SF_3$ .

It was assumed that this force component at any depth  $d_i$  may be approximated using the maximal earth pressure theory (McKyes, 1989). The soil-blade interaction and the assumed idealized earth pressure distribution on leg part of the blade are shown in Figure 3.17.

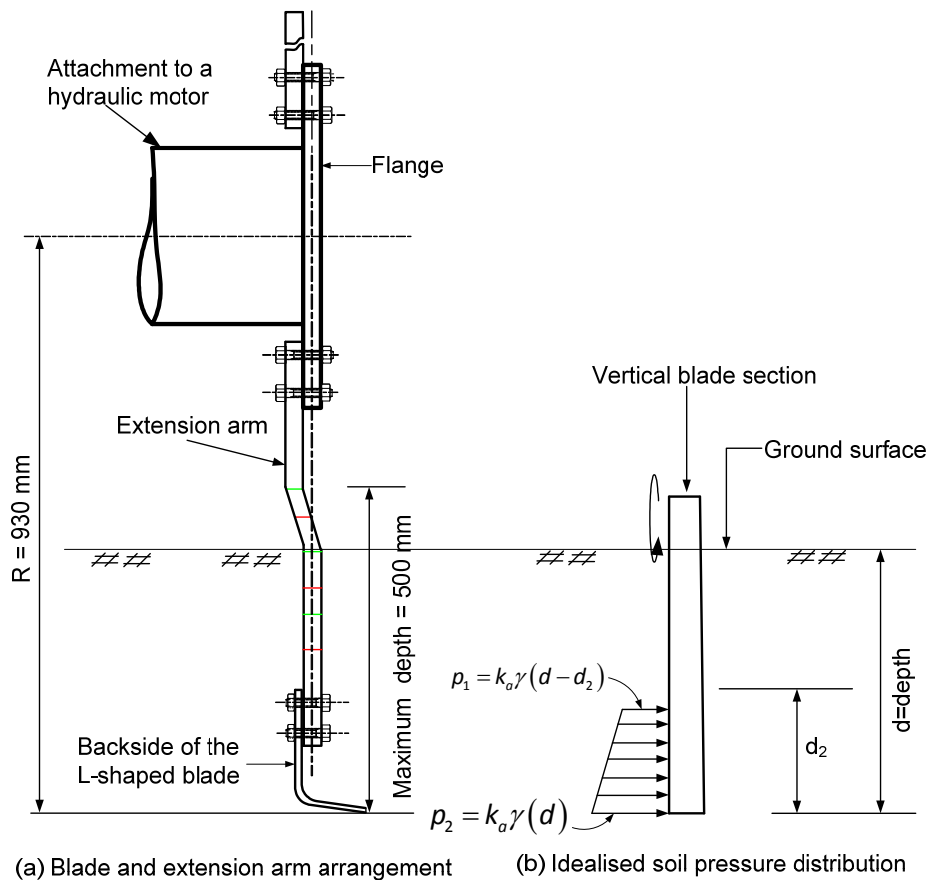


**Figure 3.17:** Idealised soil pressure distribution on the backside of the leg of the L-shaped blade

The maximum earth pressure for the distribution shown in Figure 3.17(b) at any depth  $d$ , was approximated as:

$$p_{\max} = k_a \gamma d \quad (\text{kPa}) \quad \dots (3.50)$$

The value of  $k_a$  was determined using the Rankine earth pressure theory. The value of  $k_a$  was determined using the following expression.

$$k_a = \frac{1 - \sin \phi}{1 + \sin \phi} = \tan^2 \left( 45 - \frac{\phi}{2} \right) \quad \dots (3.51)$$

Because only the backside of leg was considered to be in contact with the soil during cutting (Figure 3.17a), the average soil pressure,  $p_{ave}$ , contributing to the combined adhesive-cohesive force, was taken as the average of  $p_1$  and  $p_2$  (Figure 3.17b), i.e.,  $P_{ave} = 0.5k_a\gamma(2d - d_2)$ . It was assumed that the area of the leg contributing to this force was  $A_2$  (Figure 3.16).

The total friction and adhesion force at an instantaneous during at instantaneous time moment was calculated as:

$$\begin{aligned} SF_3 &= A_2 (C_a + p_{ave} \tan \delta) \\ &= 0.5(L \sin \beta) \left( L \cos \beta + \frac{L \sin \beta}{\tan \rho} \right) (C_a + p_{ave} \tan \delta) \quad \dots (3.52) \\ &= 0.5L^2 \times \sin \beta \left( \cos \beta + \frac{\sin \beta}{\tan \rho} \right) (C_a + p_{ave} \tan \delta) \end{aligned}$$

- *Soil-soil frictional force acting on the triangle surface abc,  $SF_2$ .* This was calculated by first determining the reaction force  $R$  on the surface. The reaction force  $R$  is given by  $R = \gamma K_o \bar{z}_c A_2$  (Perumpral *et al.*, 1983). The friction force,  $SF_2$  is then calculated from the expression

$$\begin{aligned} SF_2 &= R \tan \phi \\ &= K_o \gamma \bar{z}_c A_2 \tan \phi \quad \dots (3.53) \\ &= K_o \gamma \bar{z}_c \tan \phi \times \frac{1}{2} \left( L^2 \sin \beta \left( \cos \beta + \frac{\sin \beta}{\tan \rho} \right) \right) \end{aligned}$$

where:

$K_o$  = coefficient of lateral earth pressure at rest. In terms of friction angle of the soil,  $K_o = (1 - \sin \phi)$

$\bar{z}_c$  = depth from the top the failed wedge, i.e., points  $c$  or  $f$  to the centroid of the wedge (see Figure 3.16). The average depth at which the centroid of the wedge is from the surface of the failed soil wedge is  $\frac{1}{3} \cdot d_i = \frac{1}{3} \cdot L \sin \beta$  (m)

*The acceleration force.* The expression for the acceleration force ( $F_{acc}$ ) obtained in this study was a modified version of the one developed by Swick & Perumpral (1988). The tool velocity under rotavator soil processing is a combination of the forward travel velocity,  $V_f$  and the rotational velocity,  $V_{cir}$ . For a down-cutting rotavator blade, the instantaneous peripheral speed of any point in a cycloidal trajectory is a function of the rotor speed  $V_{cir} = R\omega$ , the forward travel speed,  $V_f$  and the distance from the rotational axis to the point of interest. In this study, this peripheral velocity was obtained using the ‘instantaneous-centre-technique’ proposed by Hendrick and Gill (1974). Using this technique, instantaneous velocity  $V$  for a down-cut operation can be calculated as:

$$V = \omega R \sqrt{\left(1 + \frac{1}{\lambda^2} - \frac{2 \sin \alpha}{\lambda}\right)} \quad \dots (3.54)$$

The modified expression for the acceleration force was of the form:

$$F_{acc} = \left(\frac{\gamma}{g}\right) \times \frac{w \times L \sin \beta \times V_i^2 \times \sin(\beta)}{\sin(\beta + \rho)} \quad \dots (3.55)$$

where:

$\gamma$  = Unit weight of the soil (kN/m<sup>3</sup>)

$g$  = gravitational acceleration,  $\approx 9.81$  (ms<sup>-2</sup>)

$w$  = tool width; which is the span of the L-shaped blade (m)

$L$  = length of the span of the blade in contact with the soil (m)

$V_i$  = the instantaneous peripheral velocity of the tool along the cycloidal path, (ms<sup>-1</sup>.)

**Derivation of the instantaneous total soil resistance force for the span ( $P_s$ )**

The total soil resisting force ( $P_s$ ) was determined by solving the equilibrium with the conditions specified in Figure 3.15. This was done by resolving the forces in the vertical (y) and horizontal (x) directions. Since the forces in the y-direction are opposite in their directions and equal in magnitudes, a 2-D representation in the x-z plane (Figure 3.18) was adequate to determine the total wedge resisting force.

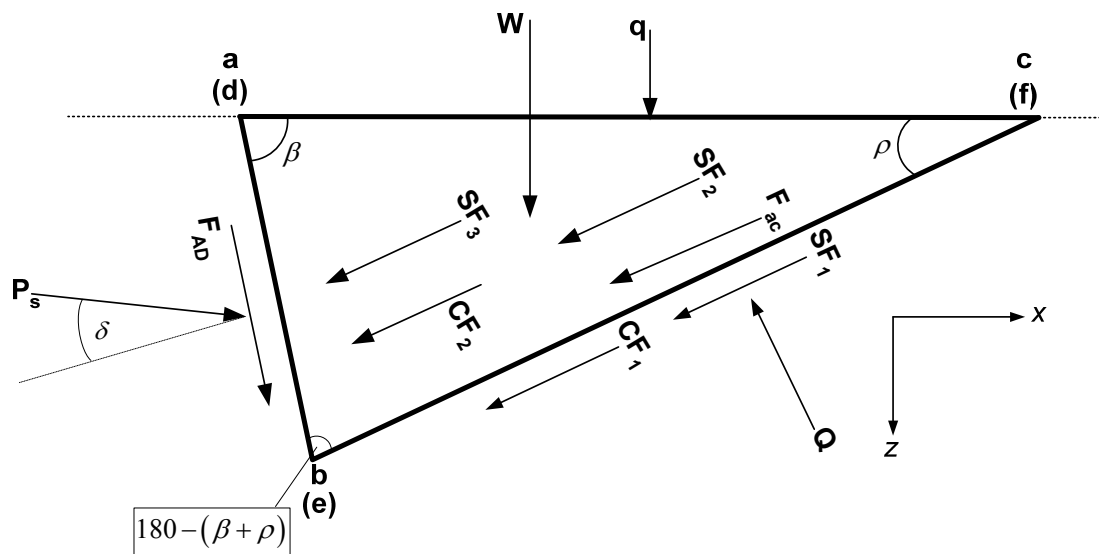


**Figure 3.18:** 2-D breakdown of the forces on the failed soil wedge

Summation of the component forces in the x- and z- directions that enabled the derivation of the total soil separation resistance due to the span as follows:

*Σ of forces in the x-direction (horizontal)*

$$\begin{aligned}
 P_x &= P_s \cos(\beta + \delta) \\
 &= -F_{AD} \cos \beta + CF_1 \cos \rho + SF_1 \cos \rho + F_{ac} \cos \rho + 2CF_2 \cos \rho \dots \\
 &\quad + SF_2 \cos \rho_2 + SF_3 \cos \rho + Q \sin \rho
 \end{aligned}
 \quad \dots (3.56)$$

*Σ of forces in the z-direction (vertical)*

$$\begin{aligned}
 P_z &= P \cos(\beta + \delta) \\
 &= W + F_q + F_{AD} \sin \beta + CF_1 \sin \rho + SF_1 \sin \rho + F_{ac} \sin \rho + 2CF_2 \sin \rho \dots \\
 &\quad + SF_2 \sin \rho + SF_3 \sin \rho - Q \cos \rho
 \end{aligned}
 \quad \dots (3.57)$$

By combining Equation (3.56) and Equation (3.57), the total soil resistance force,  $P_s$ , was obtained using the approach of Perumpral *et al.* (1983), and Swick and Perumpral (1988). The resultant equation for the total resistance force obtained was of the following form.

$$P_s = \frac{-F_{AD} \cos(\beta + \phi + \rho) + (W + F_q) \sin(\phi + \rho) + (CF_1 + 2CF_2 + SF_2 + SF_3) \cos \phi}{\sin(\beta + \delta + \phi + \rho)} \dots$$

(3.58)

The derived total separation resistance formula (Equation 3.58) is different from the one by Perumpral *et al.* (1983) only by the inclusion of the wedge weight ( $W$ ), acceleration force ( $F_{acc}$ ) and surcharge force ( $F_q$ ) terms; and the soil-metal friction force  $SF_3$  due to the presence of the leg part of the blade. It is also different from the Swick-Perumpral dynamics model expression for the centre wedge total soil separation resistance for narrow blades (Swick & Perumpral, 1988) due to the inclusion of the  $SF_2$ ,  $SF_3$ , and  $CF_2$  force terms.

In Equation (3.58), both the resistance force  $P_s$  and the soil failure angle  $\rho$  are unknown. This means that the soil resistance force  $P_s$ , the primary target in the above expression cannot be determined directly. The soil failure angle and the resistance force, however, can be determined indirectly by using the passive earth pressure theory that states that passive soil failure occurs when the resistance is minimum (Perumpal, *et al.*, 1993; Swick & Perumpal, 1988; McKyes, 1989). Consequently, either through an iteration or trial-error method, the soil resistance force  $P_s$  or the soil failure angle can be determined finding the minimum resistance value.

In this study, the approach of Perumpral *et al.* (1983) was used to solve Equation (3.58) using a computer program, written in MATLAB. The program calculates the force  $P_s$  for different values of the rupture angle as the blades processed the soil. By plotting a graph of  $P_s$  versus  $\rho$  values, the rupture angle which produces the minimum soil resistance force was selected.



### 3.4.3 Penetration resistance

During soil cutting by a rotavator, the cutting edge of the span of an L-shaped blade ( $\overline{A_2A_3}$ , Figure 3.10) continually penetrates the soil between the angles  $\alpha_i$  and  $\alpha_e$  (see Figure 3.8). This action of the blade requires torque to overcome the penetration resistance offered by the soil when the blade is moving between the two angles for any set depth of tillage. This penetration resistance was considered to be equal to the tip reaction force. The approach used to determine this tip reaction force in this study was based on the research by Thakur and Godwin (1990) in which the soil failure by the tip of the blade was demonstrated with the help of a non-extensible steel wire. The idealised system of force acting on the tip of the wire is given in Figure 3.19.

Figure 3.19 show the conceptual soil failure mechanism by a wire under two different situations, i.e., when working through a semi-infinite homogeneous soil mass, and working close to an open wall. This failure mechanism assumed to resemble the penetration of the soil by the cutting tip of the span of the blade. In the asymmetrical case near the open wall [Figures 3.19(b)], there is a general shear failure of soil towards the open wall and a local shear failure towards the infinite soil mass.

The force acting on the other half thickness of the wire [force  $RF_1$ , Fig. 3.19(b)] due to local shear failure towards the undeformed soil can be determined using the solution of Meyerhof (1951) for a wedge-shaped foundation at great depth (Thakur & Godwin, 1989; Thakur & Godwin, 1990). Based on this theory, the stress on the face of the wire for weightless soil is given as:

$$Q_s = C_c N'_c + P_o N'_q \quad \dots (3.59)$$

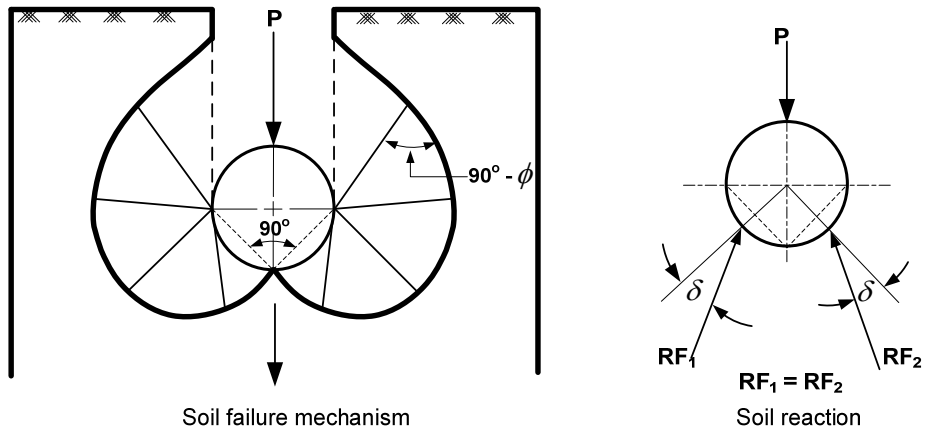
where:

$Q_s$  = force upon face of tip of the span (kN)

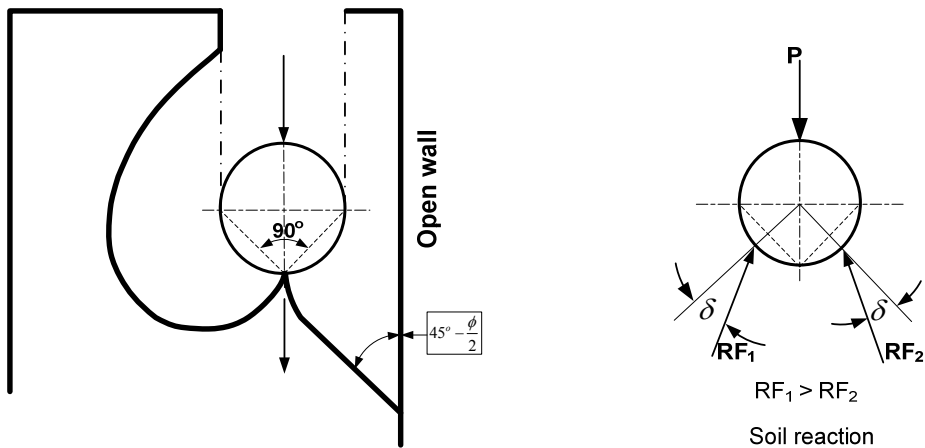
$N'_c$  = cohesion N factor

$N'_q$  = surcharge N factor

$P_o$  = geostatic stress (Pa)



(a) Symmetrical soil failure mechanism in a semi-infinite mass by a rough wedge



(b) Asymmetrical soil failure mechanism near an open wall

**Figure 3.19:** Idealized system of force acting on the tip of a wire (Thakur and Godwin (1989), after Meyerhof (1951))

The values of the dimensionless N-factors used in this study were based on the research by Meyerhof (1951) on the ultimate bearing capacity of wedge shaped foundations. Thakur and Godwin (1990) used this approach to determine these dimensionless N-factors, and obtained acceptable predicted torque requirement values for the cutting of soil by a rotating wire. For rough edges, the factors are sensibly unaffected by the wedge angle except for semi-angles of approximately less than 30 degrees, when the factors increase rapidly. In general, the N-factors for smooth wedges are much smaller than those for rough wedges. A graph of N-factors plotted by Thakur and Godwin (1990) for a wedge of  $45^\circ$  applicable to the wire (Figure 3.20) was used in this study.

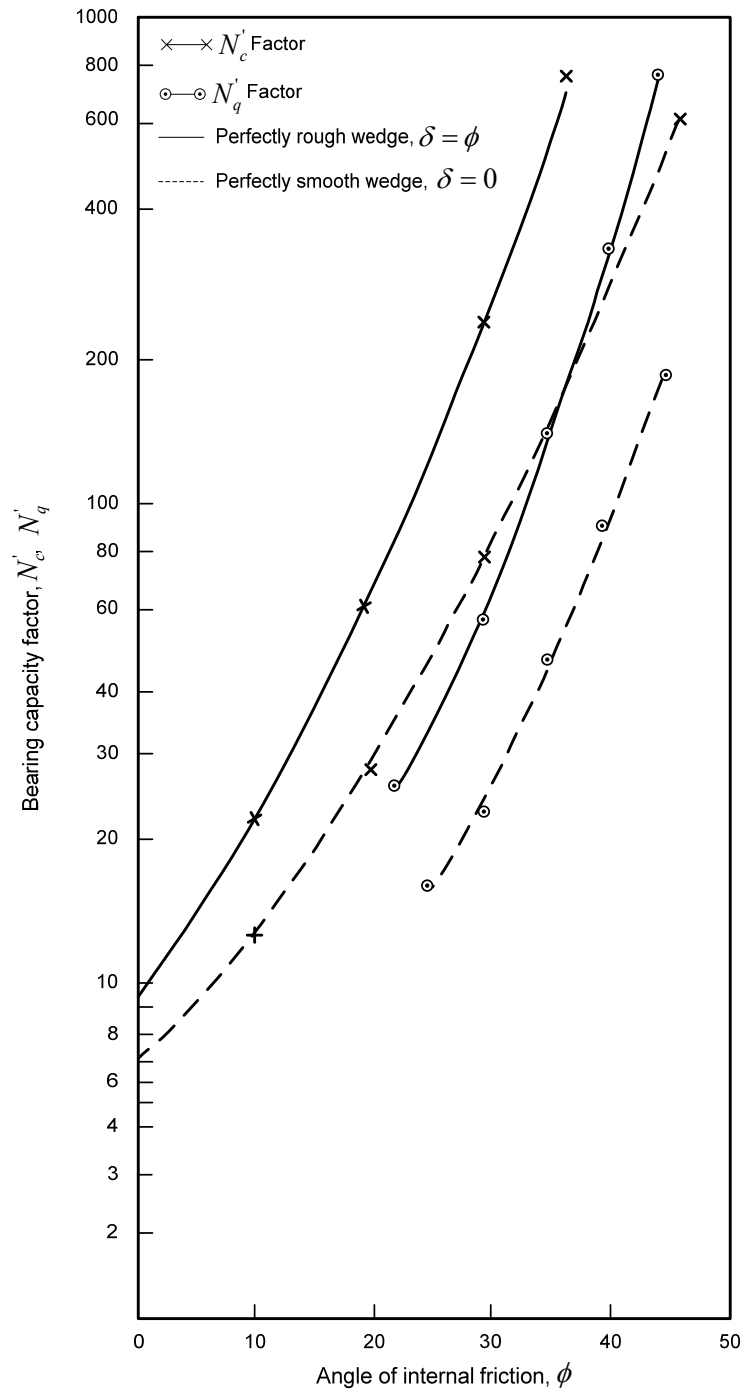


**Figure 3.20:** Relationship between bearing capacity factors and angle of internal friction for deep wedge shaped footing with included tip angle of  $90^\circ$  (Thakur & Godwin, 1989 after Meyerhof, 1951)

The geostatic stress  $P_o$  acting normal to the equivalent free surface is given by Thakur and Godwin (1990) as:

$$P_o = K_o \gamma d_i \quad \dots (3.60)$$

where:

$K_o$  = ratio of the horizontal and static vertical stress, ( $K_o = 1 - \sin \phi$ )

$\gamma$  = bulk density of the soil ( $\text{kN/m}^3$ )

$d_i$  = instantaneous depth of wire from soil surface (m)

The total force on a half thickness of the wire, considered equivalent to the thickness of the tip of the cutting edge of the span, is then obtained from the following expression.

$$P_r = \frac{t_{bt}}{2} C_c w N'_c + K_o \gamma z w \frac{t_{bt}}{2} N'_q \quad \dots (3.61)$$

where:

$C_c$  = soil cohesion ( $\text{kN/m}^2$ )

$t_{bt}$  = thickness of the cutting edge of the span of the blade (m)

$w$  = width of the span of the blade (m)

It was assumed that this tip reaction force (penetration resistance) remained constant throughout the soil cutting process by the tip of the blade as shown in Figure 3.21.

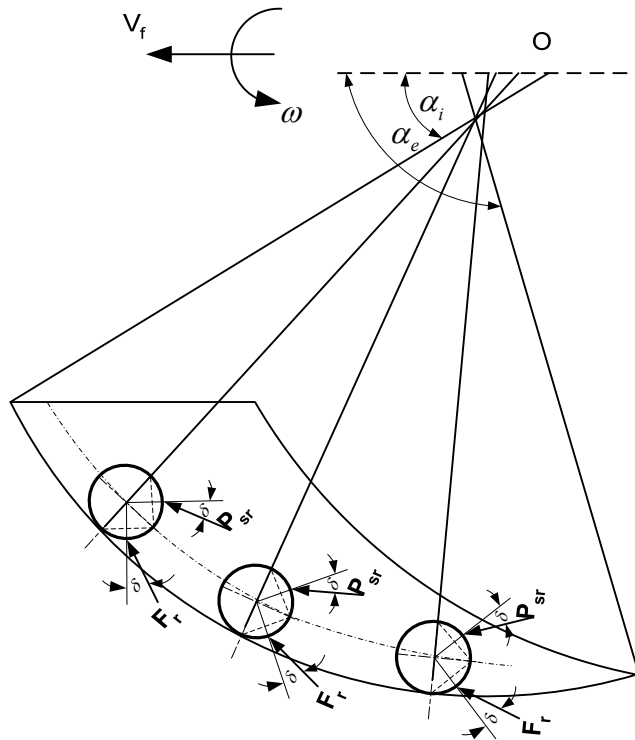


**Figure 3.21:** Soil reaction with constant tip force  $F_r$  and varying soil resistance  $P_{sr}$  for different positions of the wire in cutting a full soil slice (Thakur & Godwin, 1990)

### 3.4.5 Determination of the total torque requirements

The total instantaneous torque requirement for a single L-shaped blade is the sum of the torque due to  $P_s$  and  $P_r$ . The torque value due to these two forces is the product of the respective force and its distance from the centre of the rotor to its point of action, i.e., the centroid of the instantaneous failed soil wedge (Figure 3.16). The distances at which these two forces act are different. The  $P_r$  force acts a distance equal to the radius of the rotor at all instances during soil processing by the blade. The instantaneous time moment point of action of the force  $P_s$  is the distance from the centre of the rotor to the centroid of the instantaneous time moment soil wedge on the surface 'abcd' (Figures 3.18).

The instantaneous time moment location of the centroid of the failed soil wedge is given as  $\bar{z}_i = \frac{1}{3} \cdot d_i = \frac{1}{3} \cdot L \sin \beta$ . Given the dependence of the centroid of the soil failed by the L-shaped rotavator blade on the rake angle,  $\beta$  and the dependence of  $\beta$  on the angle turned through by the rotor,  $\alpha_i$ , from the horizontal, this parameter changes throughout between  $\alpha_{cs}$  and  $\alpha_{ce}$  when the blade is processing the soil. For any position of the rotor between angle  $\alpha_{cs}$  and  $\alpha_{ce}$ , the point of action of the location of force  $P_s$  from the centre of the rotor may be expressed as follows.

$$L_{ps} = R - \frac{2}{3} \cdot \frac{d_i}{\sin \beta} \quad \dots (3.62)$$

The instantaneous time moment torque values for the  $P_s$  and  $P_r$  may then be expressed as follows:

$$T_{ps} = P_s \cdot \left( R - \frac{2}{3} \cdot \frac{d_i}{\sin \beta} \right) \quad \dots (3.63)$$

$$T_{pr} = P_r \cdot R \quad \dots (3.64)$$

The two instantaneous time moment torque requirement values are added to give the total instantaneous time moment torque requirement as follows.

$$T_{total} = T_{ps} + T_{pr} = P_s \cdot \left( R - \frac{2}{3} \cdot \frac{d_i}{\sin \beta} \right) + P_r \cdot R \quad \dots (3.65)$$

### 3.5 Performance of the experimental tiller

The performance of tillage tools is usually determined by their draft or power requirements; and the quality of work (Srivastava, *et al.*, 1993). Quality of work is however, dependent on the types of the tillage tools; and may therefore be an unsuitable measure for the assessment of the performance of different tillage tools since this would require a common criterion. Consequently, the performance of the experimental deep tilling rotavator will be based on its draft and power requirements. Draft and power requirements of tillage tools can be manipulated to give a single performance criterion, which can be used to compare the performance of different tillage tools.

Using the draft and power requirements of tillage tools, the concept of specific energy or specific work has been used extensively (Kepner *et al.*, 1978; Srivastava *et al.*, 1993) to determine the performance of different tillage tools; including the performance of rotavators (Beeny & Greig, 1965; Beeny & Khoo, 1970). Specific energy/work is defined as the ratio of the total energy expended during soil processing by a tillage tool to the volume of the soil disturbed (Srivastava *et al.*, 1993). The specific energy or work of a rotavator may be expressed as (Beeny & Khoo, 1970):

$$\text{Specific work} = \frac{\text{Energy expended}}{\text{Volume of the soil worked}} \quad (\text{J/m}^3)$$

or

$$\text{Specific power} = \frac{\text{Power input per blade}}{\text{Volume of soil processed per blade}} \quad (\text{N.m/s.m}^3) \quad \dots (3.66)$$

The energy expended in Equation (3.65) can be determined from the product of the power and time it takes to work the volume of soil. The rotavator requires draft and rotary power when tilling the soil. The resultant draft was measured by considering the forces recorded on the two lower links and the top link of the tractor. The difference between the sum of the instantaneous time moment forces recorded at the two lower links and the top link gave the resultant thrust or pull force during rotavator operation. The energy required for both is calculated as the product of the power requirements and the time during which that power is utilised.

The rotary power requirement ( $P_{rot}$ ) may be calculated as the product of the total torque requirements (Equation 3.67) and the speed of rotor. This power requirement may be expressed as:

$$P_{rot} = \frac{\omega T_{total}}{1000} \quad \dots (3.67)$$

where:

$P_{rot}$  = power (kW)

$\omega$  = rotor speed (rad per second)

The energy required for the rotary work ( $E_{rot}$  in kNm) is then calculated as the product of the rotary power requirements and the time during which the rotary work is done. The total rotary energy expended during this time is calculated as:

$$E_{rot} = \frac{T_{total} \times \omega \times t}{1000} \quad \dots (3.68)$$

where

$t$  = time (s)

The draft energy ( $E_d$ ) is the product of the forward travel speed, the resultant (effective) horizontal draft force and the time. The draft energy component for such a force ( $E_d$  in kJ) is calculated as:

$$E_d = (V_f \times D_f \times t) / 1000 \quad \dots$$

(3.69)

where:

$V_f$  = forward travel speed (m/s)

$D_f$  = Resultant draft force (N)

The total energy expended is then the sum of the rotary and the draft energy expended during the stated time period.

The volume of the soil tilled is determined in two stages. First, the volume of the soil tilled by a single blade is calculated. Thereafter, the total volume of the tilled soil is calculated for the stated time period determined. For a single blade, the volume of the

tilled soil is given by Equation (3.35) as described in §3.2.6. Depending on the number of blades that will pass through the soil in the stated time period, the total volume of the soil worked by the tiller is calculated as:

$$V_{wsv} = z_n V_{ac} \quad \dots (3.70)$$

where:

$V_{wsv}$  = total volume of the soil tilled in time, t (m<sup>3</sup>)

$z_n$  = number of blades of the rotavator that pass through the soil in time t

$V_{ac}$  = actual soil chip volume processed by a single blade (m<sup>3</sup>)

The specific energy/work ( $SE$ ) is then calculated as:

$$SE = \frac{E_r + E_d}{1000V_{wsv}} = \frac{t(V_f D_f + \omega T_{total})}{1000V_{wsv}} \text{ kN.m/m}^3 \quad \dots (3.71)$$

Equation (3.71) can be used to compare the power performance of the experimental deep rotavator with the performance of other tillage tools. The draft component may increase or decrease the magnitude of the specific energy as the resultant draft force may be large or small, and be positive or negative with respect to the forward travel direction of the tractor.

### 3.6 Chapter summary

The kinematics of a rotavator is crucial in the development of mathematical models for predicting rotavators torque and power requirements. Rotavator kinematics influences the following parameters which have immense effect on its torque input; and thus its specific energy or power requirements.

- the cutting velocity of the tip of the span
- the cross-sectional area and volume of the soil slice,
- the equation of motion which is used to determine the location of the tip of the cutting edge of blade
- the bite length
- the kinematic parameter,  $\lambda$



- the angle at which the soil processing starts and ends by a blade
- the length of the tilling route

The analytical model for torque requirements developed for a down-cutting rotavator comprises many force elements. By combining the soil resistance forces with the motion of the rotavator blade, two categories of resistance forces that have to be overcome during down-cut rotavator tillage operation have been identified. These are the soil resistance force elements due to the soil-blade interaction; and the soil penetration resistance force. The magnitude of the forces related to the soil failure wedge is greatly influenced by the position of the blade during soil processing and the rotational and forward travel speeds of the rotavator. The penetration force on the other hand acts at a fixed distance, equal to the radius of the rotor, throughout the soil processing; and is independent of the position of the rotor.

From the derived force expressions, the torque and power requirements for a down-cutting rotavator can be calculated. The torque requirements for the blade can be calculated for different rotor positions by locating the point of action of the soil penetration resistance force and soil resistance force due to the span and leg of the L-shaped blade. Using the specific energy requirements expression, the performance of the down-cut rotavator can be compared with other tillage tools.